

# **EASTERN**

## **MICHIGAN UNIVERSITY**

---

### **LIBRARY**

## **Electronic Delivery Cover Sheet**

### **NOTICE WARNING CONCERNING COPYRIGHT RESTRICTIONS**

The copyright law of the United States (Title 17, United States Code) governs that making a photocopy or other reproductions of copyrighted materials.

Under certain conditions specified in the law, libraries and archives are authorized to furnish a photocopy or other reproductions. One of these specified conditions is that the photocopy or reproduction is not to be "used for any purpose other than private study, scholarship, or research." If a user makes a request for, or later uses, a photocopy or reproduction for purposes in excess of "fair use," that user may be liable for copyright infringement.

This institution reserves the right to refuse to accept a copying order if, in its judgement, fulfillment of the order would involve violation of copyright law.

This notice is posted in compliance with Title 37 C.F.R., Chapter II, Part 201.14.

## Method for measuring acoustic radiation fields

Gabriel Weinreich, and Eric B. Arnold

Citation: [The Journal of the Acoustical Society of America](#) **68**, 404 (1980); doi: 10.1121/1.384751

View online: <https://doi.org/10.1121/1.384751>

View Table of Contents: <http://asa.scitation.org/toc/jas/68/2>

Published by the [Acoustical Society of America](#)

---

### Articles you may be interested in

[Nearfield acoustic holography: I. Theory of generalized holography and the development of NAH](#)

[The Journal of the Acoustical Society of America](#) **78**, 1395 (1985); 10.1121/1.392911

[Sound field separation technique based on equivalent source method and its application in nearfield acoustic holography](#)

[The Journal of the Acoustical Society of America](#) **123**, 1472 (2008); 10.1121/1.2837489

[Sound-field analysis by plane-wave decomposition using spherical microphone array](#)

[The Journal of the Acoustical Society of America](#) **118**, 3094 (2005); 10.1121/1.2063108

[Evaluation of a method for the measurement of subwoofers in usual rooms](#)

[The Journal of the Acoustical Society of America](#) **127**, 256 (2010); 10.1121/1.3270392

[Acoustic centering of sources with high-order radiation patterns](#)

[The Journal of the Acoustical Society of America](#) **137**, 1947 (2015); 10.1121/1.4916594

[Plane-wave decomposition of the sound field on a sphere by spherical convolution](#)

[The Journal of the Acoustical Society of America](#) **116**, 2149 (2004); 10.1121/1.1792643

---

# Method for measuring acoustic radiation fields

Gabriel Weinreich and Eric B. Arnold

*Randall Laboratory of Physics, University of Michigan, Ann Arbor, Michigan 48109*  
(Received 13 March 1980; accepted for publication 11 May 1980)

An acoustic field which varies sinusoidally in time is completely determined by the complex values of its pressure on two concentric spheres. We have developed an experimental procedure which carries out such a measurement. If the source of sound is located inside the inner sphere, we experimentally obtain an expansion in spherical waves whose outgoing and incoming (that is, reflected) components are independently determined. This paper describes both the apparatus and the underlying theory, and presents illustrative results on the wave reflected from the wall of an anechoic chamber.

PACS numbers: 43.85.Dj

## INTRODUCTION

In connection with the study of violin dynamics, it became interesting to examine the acoustic field surrounding the instrument. At least two reasons made it so. First, different patterns of body vibration differ radically in their efficacy as radiators; specifically, a pattern whose wavelength in the violin is smaller than its wavelength in air will radiate very little, yet its amplitude can be such as to mask an underlying long-wavelength pattern which radiates considerably more. Second, the presence of an air cavity and f holes means that radiation is not only by wood motion but also by air motion, which is not directly observable.

Our work on violin radiation is in progress and will be reported separately. It seems, however, that the method of field measurement which we have developed has considerably wider applicability. This paper describes the method, along with some illustrative applications showing the type of results that it is capable of producing.

## I. THEORY

### A. Parametrization of the field

Obviously, the acoustic field has an infinite number of degrees of freedom, so that it is important to use a parametrization that takes advantage of our knowledge of field dynamics rather than simply trying to measure it everywhere. We take the acoustic pressure as the primary field quantity and represent it as an expansion in spherical waves, in which case its most general form is

$$p(r, \theta, \phi) = \sum_{L,M} [a_{LM} h_L(kr) + b_{LM} h_L^*(kr)] Y_{LM}(\theta, \phi). \quad (1)$$

Here  $p(r, \theta, \phi)$  is the acoustic pressure,  $Y_{LM}(\theta, \phi)$  a spherical harmonic, and  $h_L(kr)$  the spherical Hankel function of the first kind, defined by

$$h_L(x) \equiv (-x)^L (d/x dx)^L (e^{ix}/ix). \quad (2)$$

This function describes an outgoing spherical wave, and its complex conjugate an incoming one. Knowledge of the field then becomes equivalent to knowledge of the expansion coefficients  $a_{LM}$  and  $b_{LM}$  of the outgoing and incoming waves.<sup>1</sup>

The expansion (1) is applicable in any region lying

between two concentric spheres such that all sources and scatterers are either inside the inner sphere or outside the outer sphere. In a region where there are no sources or scatterers, the inner sphere can be eliminated; the coefficients  $a_{LM}$  and  $b_{LM}$  are then not independent of each other, but must be equal. This is so because the Hankel function is singular at the origin, but its real part, which is the spherical Bessel function  $j_L(kr)$ , is not. Physically, the equality of outgoing and incoming waves means that, with no source or scatterer inside a sphere, the outgoing waves are simply the incoming waves leaving again in the opposite direction. Experimentally, it is then sufficient to measure only one coefficient, or a known linear combination of them, for each  $L, M$ ; alternatively, measuring both provides a test of the measurement method.

Another situation in which there are not two independent coefficients for given  $L, M$  is the one in which a source is located in free space or, equivalently, in a perfect anechoic chamber. In that case  $b_{LM} = 0$  for all  $L, M$ . Indeed, the most usual procedure of anechoic chamber measurements has been to build the best chamber possible and then to ignore whatever residual reflections exist. Again, a test of such an assumption is provided by our method if all coefficients are measured.

### B. The measurement spheres

If the value of the acoustic field  $p(R, \theta, \phi)$  is known at all points on the surface of a sphere of known radius  $R$ , an expansion of this function in spherical harmonics yields the values of  $a_{LM} h_L(kR) + b_{LM} h_L^*(kR)$  for each  $L, M$ . Repeating the measurements on another sphere, we obtain a second linear combination of  $a_{LM}$  and  $b_{LM}$ , allowing the coefficients themselves to be computed. Thus the entire acoustic field is determined if its values on two concentric spheres are known. It is this fundamental fact which forms the basis of our method.

The spheres on which the field is measured should not be confused with those that limit the range of convergence of the expansion (1), and whose radii are determined by the location of sources and scatterers; the measurement spheres can be anywhere within the region of convergence. Of course, numerical errors involved in solving for the coefficients will increase if the two are very close together. Ideally, their sep-

aration should be in the vicinity of a quarter wavelength, but this quantity is not critical.

It cannot be overemphasized that this type of analysis assumes that phases, as well as amplitudes, of the field are measured. Data on amplitudes (or, equivalently, sound-pressure levels) alone are insufficient for a complete dynamical analysis of the field.

### C. Convergence of expansion

At large distances, the function  $h_L(kr)$  approaches  $\exp(ikr - iL\pi/2)/ikr$ , so that all  $L$  values behave the same except for characteristic phase shifts. For small values of  $kr$ , on the other hand,  $h_L(kr)$  becomes  $(2L - 1)!!/i(kr)^{L+1}$ . This divergent behavior, customarily described as the "near field," sets in when the argument  $kr$  becomes smaller than  $L$ . Hence, the near field extends further and further out for high  $L$ ; in fact at any  $r$ , no matter how large, near field behavior will be encountered if sufficiently large  $L$  values are included.

As far as the angular dependence is concerned, the rms values of normalized spherical harmonics are, by construction, independent of  $L$ . Of course, their oscillations become more and more rapid with increasing  $L$ , so that an experimental microphone measurement whose spatial resolution is finite will average very high  $L$  contributions to zero. This does not happen, however, until  $L$  becomes at least as large as the ratio of sphere radius to microphone size, a number much larger than the values of  $L$  dealt with in this work.

We thus see that convergence of the expansion must depend on the coefficients  $a_{LM}$  and  $b_{LM}$  falling off at high  $L$ . Now if the field is due to a source of approximate extent  $d$  located at the origin, it may be assumed that, as long as the spherical harmonic expansion of the motion of the source surface has coefficients which do not increase for high  $L$ , the radiated wave will not contain appreciable contributions for  $L$  greater than  $kd$ . The reason is precisely that for larger  $L$  values the Hankel function at the source is much larger than its asymptotic value, so that the contribution to the far field will be small. On the other hand, if the source is not at the origin, its "size" must be viewed as the radius of the smallest sphere centered at the origin which yet contains it. For example, a localized source at a distance  $R$  from the origin will have appreciable partial wave contributions up to about  $L = kR$ . In the extreme case of a plane wave (which can be viewed as due to a source infinitely far away), there is no upper cutoff on  $L$  values.

Experimentally, the presence of random errors in the measurement of amplitudes and phases of the microphone signals will appear as "white noise" in the spherical harmonic expansion, that is, it will be characterized by an essentially uniform contribution to all partial waves. If we are interested in the far field, this noise will play the same role as it does in any other physical measurement. However, if we wish to extrapolate the field inwards toward the source, a rather serious problem arises: a given amplitude of wave at

the position of the microphone will make a bigger and bigger contribution to the field at smaller radii as  $L$  increases, due to the behavior of the Hankel functions previously discussed. Thus a small but finite amount of high- $L$  noise can cause catastrophic divergences at small radii. (This is simply the converse of the fact that high- $L$  source motions near the origin do not radiate much—it is difficult to determine high- $L$  motions near the origin from measurements far away.)

What this means is that, at small radius (or, strictly speaking, at any finite radius), the expansion (1) must be viewed as semiconvergent rather than convergent, to be cut off at an  $L$  value at which the agreement with reality begins to become worse rather than better. What this value is can be estimated if we know the errors of measurement and the radii of the measurement spheres; in effect, this consideration places a limit on the resolution with which the source motion at small radius can be determined.

## II. APPARATUS AND PROCEDURE

### A. Mechanical boom system

As explained in Sec. IB, a complete determination of the acoustic field is effected by measuring the acoustic pressure on two concentric spheres. In order to accomplish this, we designed and built a special boom system which simultaneously moves two microphones so that each one maintains a constant distance from the coordinate center, and the values of the spherical angles  $(\theta, \phi)$  are always the same for both. This system must be able to locate the microphones with precision and not scatter an appreciable amount of sound. Since the first condition requires rigidity and the second small size, they are to some degree contradictory. The arrangement we have used is shown in Fig. 1. The primary boom, made of  $\frac{1}{2}$ -in. brass tubing, is pivoted at the bottom so that it can rotate about a vertical "primary" axis. Attached to it is a horizontal tube whose axis intersects the primary one. Running through this tube is the shaft of the secondary boom, at the end of which are located two Knowles BT1759 microphones, mounted so as to be radially displaced from each other. The weight of the system is supported by two thin iron wires attached to a ball bearing collar which turns on a shaft mounted to the ceiling of the room. Motion of the primary or secondary boom causes each microphone to sweep out, respectively, a "parallel of latitude" or a "meridian of longitude." Thus, the combination of the two motions allows the microphones to be placed anywhere on their respective spheres. The radii of the two measurement spheres are 58.1 and 72.6 cm.

The shafts are driven by small electric motors and worm-and-gear systems. Mounted on each final worm shaft is a Lucite disk, painted so as to have alternate opaque and transparent sectors and equipped with a pair of LED-phototransistor combinations. As the disk rotates, the square wave that comes out of the phototransistors operates a digital counting system whose state at any moment defines the position of the respective boom. The system counts up or down depending on which of the two phototransistors first sees the passing

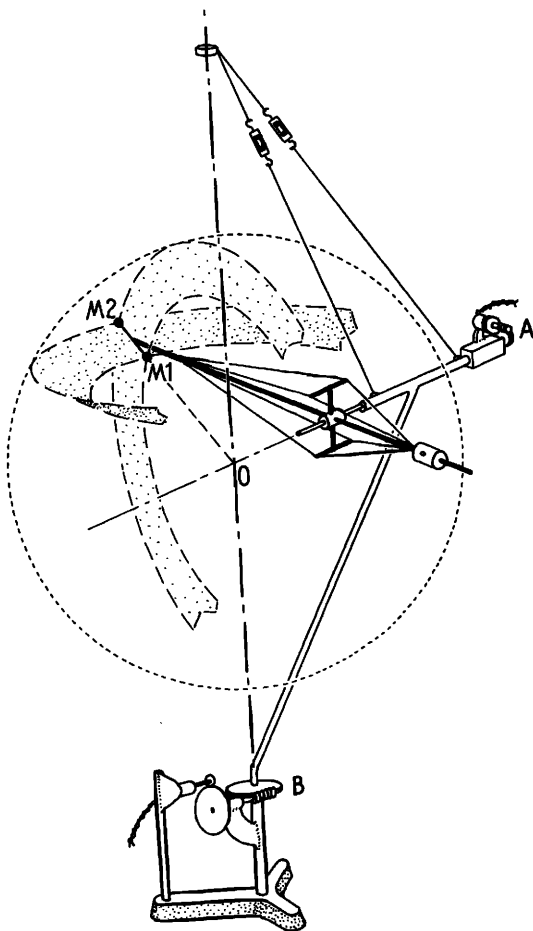


FIG. 1. Mechanical boom system. O—center of coordinate system; M1, M2—microphones; A—motor and drive for polar angle  $\theta$ ; B—motor and drive for azimuthal angle  $\phi$ .

sector edge; in this way, the position of the boom is correctly defined even though the motion reverses. The gearing is such that the 360-deg range of  $\phi$  is subdivided into 768 counts, and the 180-deg range of  $\theta$  into 400. The angular coordinates of the two microphones are, of course, always equal.

The whole system is lined up by a systematic procedure involving plumb lines, levels, and a theodolite. The final errors in locating the microphones appear to be no larger than about 5 mm on the sphere, and less than that radially.

The procedure of data taking has been to set  $\theta$  at a fixed value, sweep through a complete circle in  $\phi$ , then advance the value of  $\theta$  and repeat the process. We use 25 values of  $\theta$ , ranging from 3.6 deg to 176.4 deg in steps of 7.2 deg. The  $\phi$  sweep is begun about 30 deg before the nominal zero of  $\phi$ , allowing mechanical start-up transients to die away before significant data is taken. Similarly,  $\phi$  is allowed to run about 30 deg past the nominal end of its range, and the next circle of latitude is (after readjusting  $\theta$ ) swept in the reverse direction.

We take approximately one minute to sweep a circle of latitude. Including the above-mentioned overshoots and the time for setting the  $\theta$  values, a complete run

takes approximately 40 min.

Our interpretation of the data is, of course, valid only to the extent that the boom is acoustically transparent, so that the field does not change as the boom moves. To check the accuracy of this assumption, we used the fact that a given microphone location can be reproduced by changing the sign of  $\theta$  and adding  $180^\circ$  to  $\phi$ . The boom configuration is, however, different in the two cases, so that the scattering, if any, should be different.

Figure 2 shows data obtained in this manner. Here  $\theta$  is plus or minus  $90^\circ$ ; that is, the microphones are on the equator. The abscissa is either  $\phi$  (for the solid line), or  $\phi + 180^\circ$  (for the dashed line); hence, apart from boom scattering, the two curves should be identical. It is seen that this identity is not complete, and some boom scattering is occurring.

At least two methods could be used to decrease errors from this cause. The most obvious one is to redesign the boom structure out of thinner members, which can certainly be done. Since, however, every boom will cause some scattering, it is interesting also to ask whether the effect could be calculated so as to correct for it when the data are processed. Although we have not done it, some progress in that direction is possible if one first computes "zero-order" wave coefficients ignoring boom scattering, then uses the resulting "zero-order" field to calculate a wave scattered by the boom into each microphone. This method should be quite effective if the scattering is localized, arising, for example, from the housing of the  $\theta$  motor (which we believe to be the major scatterer now). As long as a scatterer is small compared to a wavelength, its scat-

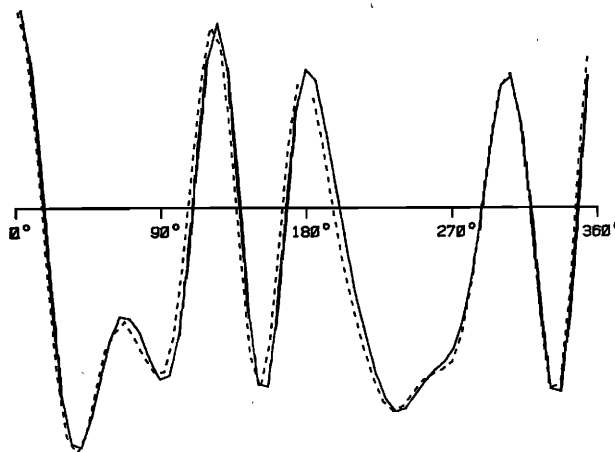


FIG. 2. Comparison of data taken in two boom configurations that correspond to identical microphone positions. What is plotted is the quadrature component of the inner-microphone signal as the microphone sweeps out the equator of the corresponding sphere, as a function of the azimuthal angle ("longitude"). The other three channels show comparable behavior. Repetition of the sweep using the same boom configuration would show deviations which are typically less than the thickness of these lines; hence, the discrepancy visible here is attributed to boom scattering. The ordinate is linear, with the maxima equal roughly to one-half of the full-scale value of the A/D converter.

tering should, in lowest order, consist only of a combination of  $s$  wave and  $p$  wave. It would be relatively easy to measure the corresponding scattering lengths empirically, and use them to compute a first-order correction to the zero-order field at the microphones and, finally, a first-order correction to the coefficients. Such a procedure should reduce errors due to boom scattering by an order of magnitude.

### B. Audio system

Figure 3 is a block diagram of the electronics, to be discussed in this and the following sections.

The oscillator used for driving the sound source must have the following characteristics:

(1) Its frequency must be very stable, since computation of the field depends on an accurate knowledge of the wavelength,

(2) It must have low harmonic content, since our analyzer circuit is sensitive to some harmonics (see below),

(3) It must provide both sine and cosine outputs to be used as references for the analyzer.

We use a specially designed oscillator which, in addition to the above features, has control inputs that allow it to be phase-locked to an external source while maintaining very low harmonic content. This makes it possible to drive a violin at a frequency which is locked to one of its string resonances, a feature which is not of direct relevance to the general method except insofar as it allows a convenient separation of the frequency stability and low distortion functions.

Amplitude and phase information is obtained from the microphone signals by an analyzer circuit which separates each of the two amplified microphone signals into sine and cosine components. This is done by producing square waves from the sine and cosine oscillator signals and using these to switch the gain of amplifiers between  $+1$  and  $-1$ . The time-average

outputs of these amplifiers are then proportional to the sine and cosine components of the original sinusoidal input. The switching is done carefully to insure a 50% duty cycle, and the positive and negative gains are accurately matched. When this is done the signal analyzers are insensitive to even-harmonic components in the input signal; odd-harmonic components do contribute in inverse proportion to their orders, however, and thus must be minimized in the input signal if possible. The signal analyzer outputs are filtered by second-order, critically damped low-pass filters with 10-Hz corner frequencies which effectively average over many cycles of the signal analyzer outputs.

The sensitivities of the two microphones, as well as the gains in the associated amplification and analyzing channels, were intercalibrated by repeating some typical runs after physically interchanging the two microphones.

The four filtered outputs of the signal analyzer, which are slowly varying dc voltages, are routed next to four analog sample/hold amplifiers, based on the Analog Devices model AD582 integrated circuit, and controlled by logic circuits which cause the HOLD mode to be entered when an externally generated FREEZE signal is received (see next section). The logic circuits then insure that the HOLD mode is maintained as long as is necessary to digitize all four sampled signals and store the resulting digital values in temporary storage registers. Following this, the sample/hold circuits return to the SAMPLE mode, in which they quickly acquire the current values of the signal analyzer outputs and follow them until the next FREEZE signal occurs. If a FREEZE signal occurs while the previously held values are still being digitized, an inhibiting signal is produced which prevents it from propagating to other parts of the logic circuitry which depend on it to perform other functions simultaneously with the sampling of the signal analyzer outputs. When the digitizing has been completed, this inhibiting signal is removed after a short delay (to permit the sample/hold circuits to settle to new values) and the FREEZE signal propagates in its normal manner

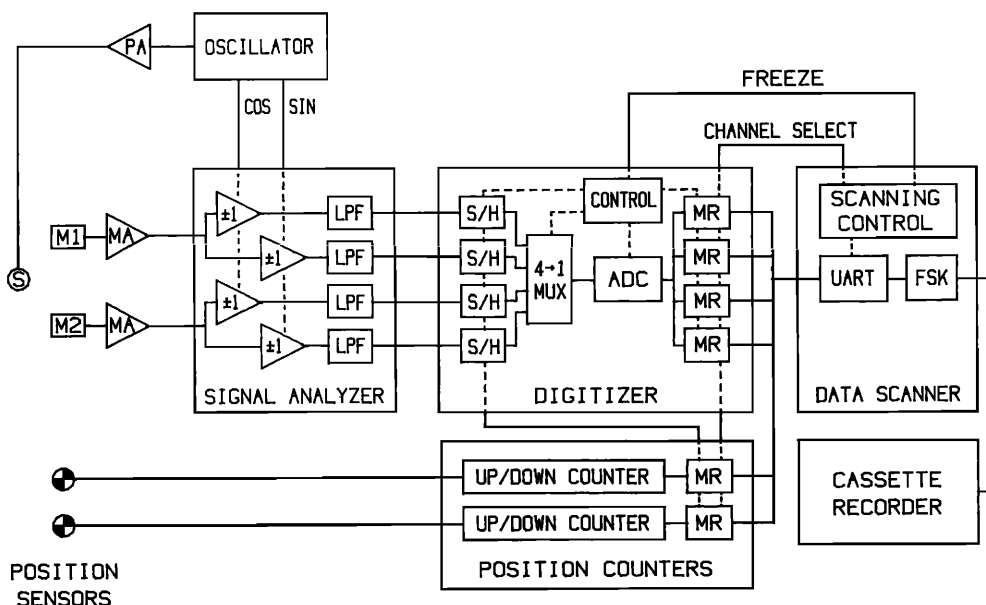


FIG. 3. Block diagram of the electronics. PA—power amplifier; S—sound source; M1, M2—microphones; MA—microphone preamplifiers; LPF—low-pass filters; S/H—sample/hold amplifiers; MUX—multiplexer; ADC—analog/digital converter; MR—memory registers; UART—ASCII serial code generator; FSK—modulator.

to cause the newly acquired analog values to be held again.

The four sample/hold outputs are multiplexed by a tree of Analog Devices model AD7512 SPDT analog switches. The multiplexed output goes directly to the analog input of the A/D (analog-to-digital) converter, which is an Analog Devices model AD7550 integrated circuit. This is a fairly slow, 13-bit device that uses a conversion technique that minimizes many potential errors without requiring component trimming adjustments. A very stable reference voltage is provided by a National Semiconductor type LM3999Z integrated circuit, a device that has a built-in heater and temperature regulator which lower the dependence of the reference voltage on the ambient temperature by an order of magnitude over the best temperature-compensated Zener reference diodes, and at much lower cost. It produces a reference voltage of about 7 V, which gives the A/D converter full-scale values of about 3.28 V, or about 0.8 mV/LSB (least significant bit) for the resolution of the digitizer. Test measurements made by introducing sine and cosine signals from the sine wave oscillator into the signal analyzer inputs give sample standard deviations of 0.54 to 1.1 LSB, so the system is capable of making measurements significant down to the LSB. The A/D converter can operate at a maximum rate of about 25 conversions per second, but at somewhat reduced accuracy. A compromise between speed and accuracy resulted in a conversion rate of about 10 per second, at which the standard deviations noted above were obtained. This rate is fairly practical when considered as part of the remaining data transmission system, which is described below. If only the digitized values of the analog signals are transmitted, then the speed of data collection is limited by the A/D converter, but when more data (such as the position of the microphone boom) is transmitted, this is no longer the case. The amount of additional data transmitted for the sound-field measurements puts this system near its optimal operating point, with the A/D converter busy essentially all of the time, but with other data being transmitted while the converter is producing its four digitized outputs.

### C. Data recording system

During the  $\phi$  sweep, which takes place continuously, the counters give the instantaneous position of the microphones, and the four analyzer outputs give the values of the real and imaginary parts of the two microphone signals. Strictly speaking, the analyzer outputs must be regarded as being delayed by approximately 0.03 s due to the filter time constants. However, at the sweep speed we use, the microphones never move more than a millimeter or two during this period, causing only a negligible error.

The data recording is supervised by a data line scanner circuit, whose cycle consists of the following steps:

(1) A FREEZE signal is sent to the counters and analyzers, causing the counters to save their states in

storage registers, and the analyzers to save their outputs in the four sample-and-hold amplifiers. The counters themselves continue to count, of course, since the motion of the boom is not stopped.

(2) The same FREEZE signal causes the contents of the sample-and-hold amplifiers to be digitized and the digital results saved.

(3) The line scanner interrogates the six data registers in turn, receiving from each register thirteen bits of data and one additional bit which is either an overflow bit from the A/D converter or a directional bit from the counters indicating the sense of boom motion. Each set of 14 bits is concatenated with four bits identifying the data register from which it was received, and the resulting 18 bits are coded serially at 300 baud as a "syllable" of three ASCII characters each in the range 040-137 octal.

(4) The sequence of six "syllables" has appended to it a (CARRIAGE RETURN)-(LINE FEED)-(NULL) sequence which terminates a line of data and simultaneously releases the FREEZE signal so that the circuits can acquire the next data value.

(5) The serial ASCII is converted to a standard FSK-modulated audio signal and recorded on an ordinary audio cassette recorder, after which the cycle begins anew.

The whole cycle could in principle be done in 0.7 s (21 characters at 300 baud), but in fact takes about 1 s because the line scanner must wait for the A/D converter to complete its task. At this rate, each circle of latitude comprises 50 to 60 points of data. On the equator, this density in  $\phi$  is consistent with the spacing that we are using in  $\theta$ ; at higher latitudes, we obtain more points than necessary.

The temperature of the air was measured both before and after each run and the average value used in the data reduction (the change was seldom more than 0.2 °C).

The complete cassette tape from a run was, at a later time, read into the central computer of the University of Michigan Computing Center via a 300-baud dial-up link, and stored as a disk file for later analysis. The reading-in process was occasionally unsuccessful because, playing from an audio cassette, there is no way to stop and start the data transmission in response to XON and XOFF signals from the computer. As a result, data could be lost if, during a busy time-sharing period, the computer input buffer overflowed before it was emptied. This did not happen often and, when it did, we were made clearly aware of it by appropriate error messages; in such a case, the transmission process was repeated. We are now converting to a floppy-disk system which not only can be better controlled, but is also capable of transmitting to the computer at a higher data rate, so that a 40-min run will not require another 40 min to be read in. The original system had the considerable advantage of low cost, however; it was put together, mostly as homemade circuitry, for approximately \$300.

#### D. Computer processing

The data collected in the manner described in the preceding section is, for each microphone, expanded in spherical harmonics up to  $L = 9$ . If  $F(\theta, \phi)$  is the complex amplitude of the microphone signal (which is proportional to the complex acoustic pressure), the coefficient  $C_{LM}$  of this expansion is obtained from the original data,  $F(\theta, \phi)$ , by

$$C_{LM} = \int_0^\pi \mathcal{P}_{LM}(\theta) G(M; \theta) \sin\theta d\theta, \quad (3)$$

where

$$G(M; \theta) = (2\pi)^{-1/2} \int_0^{2\pi} \exp(-iM\phi) F(\theta, \phi) d\phi. \quad (4)$$

Here  $\mathcal{P}_{LM}(\theta)$  is a normalized associated Legendre function. The computing procedure is straightforward: since the data file runs through a complete circle in  $\phi$  at constant values of  $\theta$ , we first compute the functions  $G(M; \theta)$  on each circle. This is done by direct numerical integration, assigning an increment  $d\phi$  to each point by examining the preceding and following values of the independent variable. In this way, 19 values of  $G(M; \theta)$ , with  $M$  ranging from  $-9$  to  $+9$ , are found for each  $\theta$ . At the end of every  $\phi$  sweep the program computes contributions to the 100 integrals  $C_{LM}$  using appropriate values of the functions  $G(M; \theta)$ .

Having obtained the spherical harmonic expansion of the acoustic field on each sphere, it is a simple matter (knowing the radii, the frequency, and the speed of sound) to obtain the coefficients of the incoming and outgoing waves. After that, the field at any location in the region of convergence can be computed, either as an acoustic pressure or as any desired component of velocity. We have found it extremely useful to plot the results with the use of a Hewlett-Packard 7221A digital plotter. Some examples are given in the discussion of the next two sections.

### III. ILLUSTRATIVE RESULTS

#### A. A plane wave

As stated above, whenever there is no source or scatterer inside the measuring spheres, the coefficients of the outgoing and incoming waves must be equal so as to add up to the nonsingular Bessel function. Preliminary tests, with the apparatus in an ordinary laboratory with considerable wall reflections, showed that condition to be rather well satisfied. It seemed interesting, however, to repeat the experiment in an anechoic chamber, where we could deal with a wave which not only originates outside the measuring spheres, but whose nature is fairly well known. In particular, a plane wave propagating in the direction  $\theta', \phi'$  has the expansion

$$4\pi \sum_{LM} i^L j_L(kr) Y_{LM}^*(\theta', \phi') Y_{LM}(\theta, \phi), \quad (5)$$

showing that arbitrarily high  $L$  values will be represented in it. If the wave is not exactly plane, but originates from a localized source some distance  $R$

away, it is easily shown that its expansion will match that of a plane wave for  $L$  values up to about  $kR$ .

With the boom system assembled and lined up in the center of the anechoic chamber, we placed a loudspeaker in one of the corners of the room, at a distance of 2.77 m from the center of the spheres defined by the measuring system. Choosing a frequency of 733.5 Hz (because of the accidental availability of a crystal-controlled source at that frequency), we find that the resulting wave should be essentially plane up to  $L = 35$  or so. Since our analysis never went beyond  $L = 9$ , the approximation to a plane wave should be excellent.

Having taken a complete run under these circumstances, we first computed the coefficients of outgoing and incoming waves. The amplitudes of the two waves were then separately resynthesized at large radii, omitting the factors  $\exp(\pm ikr)/ikr$  which characterize the radial dependence of the far field. The results are shown as polar plots in Fig. 4. The plane of the diagrams is vertical and is oriented so as to include the loudspeaker, the dotted lines showing the direction in which it is located.

For an ideal plane wave, the outgoing wave should

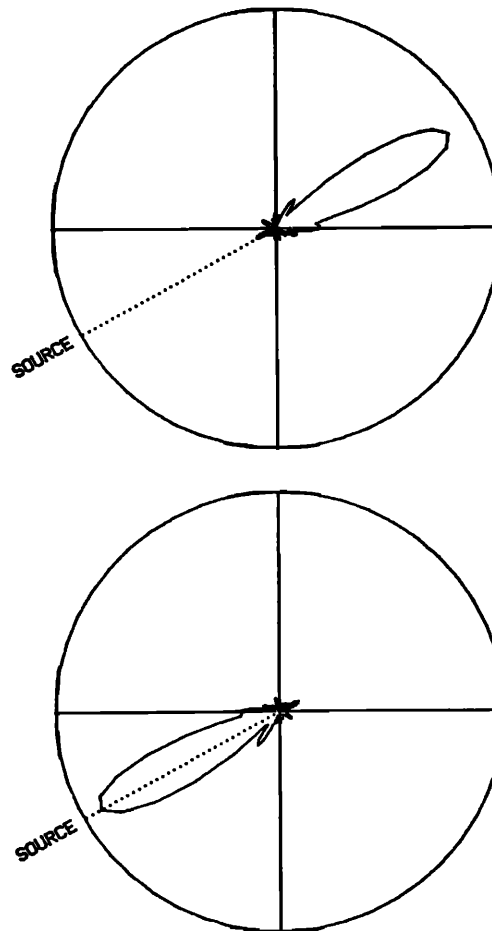


FIG. 4. Separation of an almost-plane wave into outgoing (top) and incoming (bottom) parts. The absolute value of the reconstructed asymptotic amplitude at large distances is plotted in a polar graph in a vertical plane, oriented so as to contain the source (whose direction is indicated by the dotted lines). The summation of spherical harmonics is carried up to  $L = 9$ .

appear as a delta function in the direction of propagation, and the incoming wave as a delta function in the opposite direction. Insofar as the wave is more complicated than merely plane, the pattern can change, but the incoming and outgoing waves must remain inversion images of each other as long as there are no sources or scatterers inside the measuring spheres. It is seen that the results are in excellent agreement with this expectation. The finite width of the lobes is consistent with the fact that we expand only up to  $L = 9$ .

### B. Anechoic chamber reflections

As one of the applications of our method, we examined the wave reflected from the wall of our anechoic chamber. This chamber is part of the University of Michigan Phonetics Laboratory, and its construction has been described elsewhere.<sup>2</sup> For the present purpose, it is important to note that the structure of the walls is different from the wedge arrangement commonly used. As a money-saving feature, the chamber was built instead with accordion-like walls made by lacing a fiberglass blanket in and out between a grid of metal bars approximately 2 ft apart. The rods are vertical on the walls but, of course, horizontal on the ceiling and floor, and the depth of the accordion is approximately equal to its spacing.

In order to interpret the incoming wave in terms of the properties of the chamber, it is convenient to have the outgoing wave as simple as possible, preferably isotropic. We produced sound at a frequency of 733.5 Hz by a pair of inexpensive 2¼-in. speakers mounted at the ends of a 3-in.-long tube of the same diameter, and wired so that the outward motions of the two cones are in phase. This pseudoisotropic source was mounted

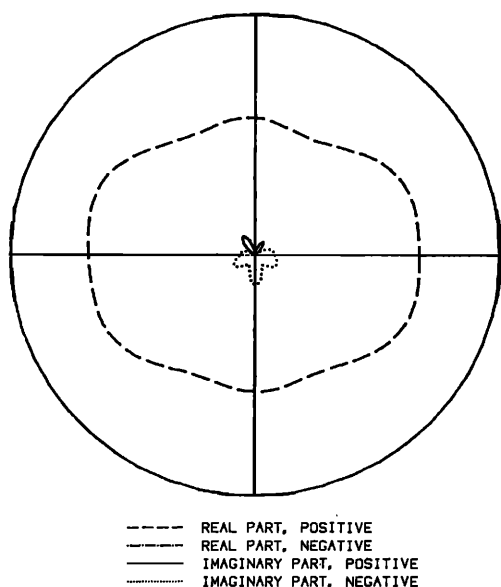


FIG. 5. Outgoing wave from a double-loudspeaker source at the center of the measurement spheres, plotted as a reconstructed asymptotic amplitude at large distances. The plane of the (polar) plot is horizontal. The phase is shown by plotting the real and imaginary parts separately, and using different dashed-line fonts to distinguish positive and negative values.

at the center of the spheres defined by the microphone motion, and a run was taken.

Figure 5 shows the result for the outgoing wave, plotted in a horizontal plane as the amplitude which would obtain asymptotically at large distances from the source [after taking out the factor  $\exp(ikr)/ikr$ ]. In this case the phase is indicated by drawing the real and imaginary parts of the amplitude separately, and further distinguishing positive from negative values by the choice of dashing fonts. It is seen that the pattern, while not exactly isotropic, is at least devoid of any fine structure that would make the interpretation of the reflected wave difficult. The imaginary part of the amplitude, which is positive in the forward direction and negative in the backward one, is due to imprecise centering of the source relative to the coordinate system of the microphones and the fact that the responses of the two speakers at this frequency are not completely identical.

The reflected wave is shown in Fig. 6, on a scale which is magnified by a factor of ten (that is, 20 dB) relative to Fig. 5. The pattern is easily explained as due to diffraction of the sound from the periodic accordion-shaped walls. In fact, the numbered lines in the figure indicate the directions of the zero-, first-, and second-order peaks to be expected from geometrical considerations of wavelength and accordion spacing. It is also interesting to note that the size of the lobes is consistent with the fact that the wall, viewed as a grating, is "blazed" for second order at this frequency; that is, the accordion angles are such that specular reflection occurs at approximately the second-order angle.

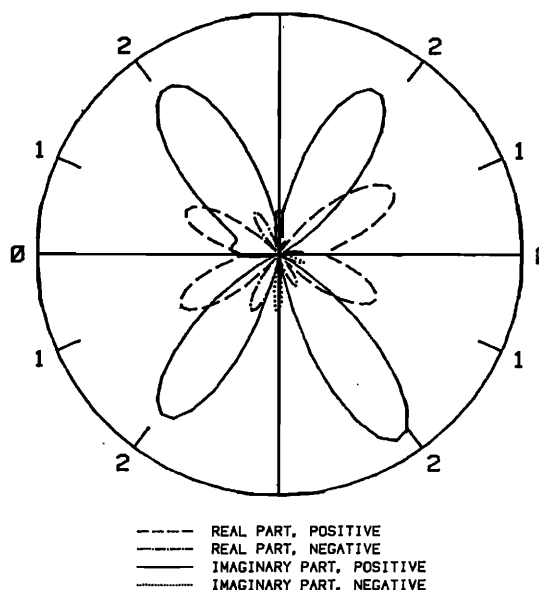


FIG. 6. Incoming wave obtained from the same run as Fig. 5, and due to reflection of the outgoing wave from the wall of the anechoic chamber. The scale represents a magnification of a factor of ten, or 20 dB, relative to Fig. 5. The numbered segments on the circumference of the graph indicate the location of diffraction maxima of corresponding order, as computed directly from the geometry of the accordion-shaped walls.

#### IV. CONCLUSIONS

The method described in this paper allows an analysis of acoustic fields at a level of detail not heretofore available. Considerable improvements, both in the mechanical boom structure and in the data processing, are still possible. In connection with the latter, a fast system which digitizes the microphone waveforms themselves could be combined with a broadband source and Fast Fourier Transform procedures to obtain data at many frequencies simultaneously.

Although our main interest was in violin acoustics, it appears that the domain of applicability of the method is much wider.

#### ACKNOWLEDGMENTS

This work was supported in part by National Science Foundation grant number PHY77-22953. We are

grateful to Sarah Gilbert, Jack Bartholomew, Lillian Ho, and John Monforte for help with experimental procedures, and to Tom Witten, Michael Sanders, and Colin Gough for fruitful discussions of various aspects of the work.

<sup>1</sup>For a discussion of spherical harmonics and spherical Hankel functions see, for example, G. Arfken, *Mathematical Methods for Physicists* (Academic, New York, 1970), 2nd ed., Chaps. 11-12.

<sup>2</sup>G. W. Peterson, G. A. Hellwarth, and H. K. Dunn, *J. Audio Eng. Soc.* **15**, 67-72 (1967).